A COMPARISON OF THE AXISYMMETRIC AND PLANAR ELONGATIONAL VISCOSITIES OF A POLYMER

Peter Beaupre and Mahesh Gupta
Mechanical Engineering-Engineering Mechanics Department
Michigan Technological University
Houghton, MI 49931

Abstract

The elongational viscosities of a low density polyethylene in axisymmetric and planar flows are compared. The experimental data on entrance pressure loss is matched with the corresponding finite element predictions to estimate the parameters in the elongational viscosity model proposed by Sarkar and Gupta. The entrance losses in the capillary and slit rheometers are used to predict the elongational viscosities for axisymmetric and planar flows respectively. The power-law region of the axisymmetric as well as planar elongational viscosity is found to follow the time-temperature superposition principle.

Introduction

Flows in various polymer processing techniques range from highly shear dominated in processes such as injection molding and transfer molding to highly elongation dominated in extrusion, thermoforming and blow molding. In the processes with elongation-dominated flows, elongational viscosity has a large effect on the velocity and pressure distributions. Therefore, an accurate knowledge of the elongational viscosity is critical for flow simulation and for optimum design of the equipment required for these processes.

The procedure for measurement of the shear viscosity of a polymer is well established [1]. Typically, a cone and plate viscometer is used to measure the viscosity at low shear rates, whereas at high shear rates the viscosity is measured by using a capillary or a slit rheometer. The experimental data from capillary (axisymmetric flow) and slit (planar flow) rheometers show that the shear viscosity for the axisymmetric and planar shear flows is the same. Several empirical equations [2, 3, 4] are available in the literature, which can accurately capture the shear-rate and temperature dependence of the shear viscosity of various polymers.

Measurement of the elongational viscosity of polymers is still an actively explored topic. Various techniques for direct experimental measurement of the elongational viscosity of a polymer, such as uniaxial extension, lubricated compression, fiber spinning, bubble collapse, stagnation flow using a four-roll mill or opposing jets etc, can be used to measure the elongational viscosity only at low elongation rates (< 10 s^{-1}), because maintaining a steady extensional deformation is difficult at higher elongation rates [5]. Furthermore, these techniques are typically used to measure axisymmetric elongational viscosity; which can be different than the viscosity for a planar elongational flow [6]. Due to these difficulties associated with direct measurement of the elongational viscosity of a polymer, entrance flow is used in this paper to estimate the planar as well as the axisymmetric elongational viscosity of a polymer.

Dependence of Elongational Viscosity on Elongation Mode

For a purely elongational flow, the strain-rate tensor, $(\tilde{e} = (\nabla \hat{v} + \nabla \hat{v}^T)/2)$, where $\hat{v}$ is velocity, is as follows:

$$\tilde{e} = \dot{\varepsilon} \begin{bmatrix} 1 & 0 & 0 \\ 0 & -(b+1)/2 & 0 \\ 0 & 0 & (b-1)/2 \end{bmatrix} \quad (1)$$

where $\dot{\varepsilon}$ is the elongation rate and the parameter b specifies the nature of the elongational flow, with $b = 0$ for an axisymmetric flow and $b = 1$ for a planar flow. A mixed elongational flow is obtained for b between 0 and 1.

In contrast to the shear viscosity (η_s), the elongational viscosity (η_e) of a fluid depends upon the elongation mode. For Newtonian fluids, for an axisymmetric flow $\eta_e = \eta_{ea} = 3\eta_s$, whereas for a planar flow $\eta_e = \eta_{ep} = 4\eta_s$. Dependence of the elongational viscosity of a polymer on elongation mode is explored later in this paper.

Entrance Flow Method for Elongational Viscosity Estimation

Entrance flow refers to the flow in a channel with an abrupt contraction. Because of the large elongational deformation experienced by the fluid near an abrupt contraction, a sharp pressure drop, called entrance loss, is encountered near the contraction. The entrance loss increases as the elongational viscosity is increased [7]. Since the entrance loss also depends upon the flow rate in

the channel, it can be used for an indirect measurement of the strain-rate dependence of the elongational viscosity of a polymer.

By adding the pressure drop due to shear and elongational deformations near an abrupt contraction, Cogswell [8] was the first to obtain an estimate of elongational viscosity using the entrance pressure loss near an abrupt contraction. To simplify the analysis, Cogswell made several assumptions that were listed in our earlier publication [9]. Because of its simplicity, Cogswell's expression is commonly used in the plastic industry to estimate the elongational viscosity of a polymer. Binding [10] removed some of the assumptions in Cogswell's analysis and employed the energy principle to obtain a more accurate expression for entrance loss in terms of the power-law parameters for the shear $(\eta_s = A\dot{\gamma}^{n-1})$ and elongational $(\eta_e = B\dot{\gamma}^{m-1})$ viscosities, and the flow rate in the channel:

$$\Delta p_e = \frac{k_1 A (1+m)^2}{m^2 (1+n)^2} \left[\frac{k_2 m B n^m I_{nm}}{A} \right]^{\frac{1}{m+1}} \quad (2)$$

$$\times \dot{\gamma}_w^{\frac{m(n+1)}{m+1}} \left[1 - \alpha^{\frac{k_3 m(n+1)}{m+1}} \right]$$

where the parameters $k_1, k_2, k_3, \alpha,$ and $\dot{\gamma}_w$, given below, are different for the planar and axisymmetric flows.

	Axisymmetric flow	Planar flow
k_1	$2/3$	$1/2$
k_2	$3n+1$	$2n+1$
k_3	3	2
α	R_0 / R_1	H_0 / H_1
$\dot{\gamma}_w$	$\dfrac{(3n+1)Q}{\pi n R_0^3}$	$\dfrac{(2n+1)Q}{2dn H_0^2}$

where $R_0 (H_0)$ and $R_1 (H_1)$ are the radii (heights) of the downstream and upstream channels respectively, Q is the flow rate and d is the width of the slit in the planar case. In Eqn. (2), I_{nm} is determined from the following equation

$$I_{nm} = \int_0^1 \left| k_2 \rho^{1+1/n} / n - k_4 \right|^{m+1} d\rho$$

where $k_4 = 2$ for an axisymmetric flow and $k_4 = 1$ for a planar flow. Even though more accurate than Cogswell's analysis, Binding's analysis is also based upon several simplifying assumptions, which were also listed in reference [9].

By relaxing all other assumptions, except for the assumption of an inertia-less, incompressible flow with no normal stresses in shear, Gupta [9] recently obtained estimates of the axisymmetric elongational viscosity of a

low density polyethylene (Dow 132i) at 160 and 175°C. For simulating the entrance flow, Gupta [9] employed the finite element method along with the Carreau model for shear viscosity:

$$\eta_s = \eta_0 (1 + (\lambda e_{II})^2)^{\frac{n-1}{2}} \quad (3)$$

and the model proposed by Sarkar and Gupta [10] for elongational viscosity

$$\eta_e = \eta_0 \left[T_r + \delta \left\{ 1 - \frac{1}{\sqrt{1 + (\lambda_1 e_{II})^2}} \right\} \right] [1 + (\lambda_2 e_{II})^2]^{\frac{m-1}{2}} \quad (4)$$

where e_{II} is the second invariant of the strain-rate tensor, T_r, the Trouton ratio at low shear rates, is 3 for an axisymmetric flow and 4 for a planar flow, and $\eta_0, \lambda, n, \delta, \lambda_1, \lambda_2$ and m are material dependent parameters. The same approach, which is discussed briefly in the next section, is used in this paper to estimate the axisymmetric as well as planar elongational viscosity of Dow 132i.

Procedure for Estimation of Elongational Viscosity Parameters

In the present work, following the approach used by Gupta [9], the elongational viscosity of a polymer is estimated by optimizing the four parameters $\delta, \lambda_1, \lambda_2$ and m in Eqn. (4) such that the difference between the entrance loss predicted by a finite element simulation and the corresponding experimental values at various flow rates is minimized. The optimization scheme used for the results reported in this paper is the same as the scheme used in reference [9]. In this scheme, for a good computational efficiency instead of using all entrance loss vs. flow rate data points, a systematic scheme, described in detail in reference [9], is employed to select four of the data points for estimation of the four elongational viscosity parameters. In particular, two data points at high flow rates are used to estimate the power-law parameters λ_2 and m, whereas a point at a low flow rate is used to estimate λ_1 and another point at an intermediate flow rate is used to estimate δ. As described in reference [9], first, the optimal values of λ_2 and m are determined by using the Newton-Rapson method [12] alternately for the two parameters. Using the data point identified for optimization of the δ parameter, the Newton-Rapson method is used again to estimate the value of δ. Finally, the parameter λ_1 is estimated by using the bracketing and bisection technique [12] to minimize the error for the data point identified for λ_1 optimization.

Experimental Data

A Goettfert Rheograph 3000 was used to measure the shear viscosity and entrance pressure loss for the planar

geometry. A slit die with a pressure transducer located in the reservoir before the contraction and three transducers located at 30, 55 and 80 mm downstream from the contraction was used. The height and width of the die opening were 0.5 and 10 mm, respectively. The pressure readings from the three transducers along the die were extrapolated till the abrupt contraction. The difference between this extrapolated value of pressure and the pressure reading from the transducer located in the reservoir is the entrance loss.

A Goettfert Rheotester 1000 was used to measure the shear viscosity and entrance pressure loss for the axisymmetric case. Three dies with a capillary diameter of 1mm and capillary lengths of 5, 20 and 30 mm were used. The pressure vs. capillary length curves were extrapolated to find the entrance pressure losses for various flow rates. This entrance pressure loss data was also used to make the Bagley correction for shear viscosity measurement.

For axisymmetric as well as planar flow, the Weissenberg-Robinowich correction was performed to account for the effect of a non-parabolic velocity profile on shear viscosity measurement. The entrance pressure loss vs. flow rate data was plotted on a log-log graph. A fourth order interpretation was used to fit a curve to the experimental data, which was then used to obtain the data points for the finite element simulations.

A Bohlin VOR with 25mm parallel plates was used to measure the shear viscosity at low shear rates and the Arrhenius equation was used to find the zero shear rate viscosity at specific temperatures. The polymer used was a low density polyethylene (Dow 132i). Data was taken for two temperatures, 215 and 230 $^\circ$C.

Results and Discussion

The experimental data on shear viscosity of Dow 132i and the curve, which is obtained by fitting the Carreau model to the experimental data, are shown in Fig. 1. For the curves shown in the figure, the Carreau model parameters are as follows:

215°C: $\eta_0 = 1.24 \times 10^5$ Pa.s, $\lambda = 63.3$ s, $n = 0.401$
230°C: $\eta_0 = 1.05 \times 10^5$ Pa.s, $\lambda = 53.6$ s, $n = 0.401$

It is noted that the power-law index reported above is different than the value of the index reported in reference [9] for the shear viscosity at 160 and 175°C. The shear viscosity parameters reported in reference [9] were based upon the experimental data obtained by using a capillary rheometer at Michigan Technological University. The data obtained by using a slit rheometer at Datapoint labs [13], resulted in a slightly different estimate of the shear viscosity. The Carreau model parameters reported above, which are based upon the data from the slit rheometer, have been used for all the results reported in this paper.

For axisymmetric and planar flows of Dow 132i, Figs. 2 and 3 respectively, show the experimental data for

entrance loss at two temperatures. The Carreau model for shear viscosity shown in Fig. 1 along with the entrance loss data in Figs. 2 and 3 were used to predict the axisymmetric and planar elongational viscosities, respectively.

For the axisymmetric flow the channel contracted from 12 mm to 1 mm in diameter, whereas for the planar flow the channel height contracted from 12 mm to 0.5 mm. Therefore, different finite element meshes were used to simulate the axisymmetric and planar entrance flows.

As mentioned earlier, the elongational viscosity estimation procedure starts with optimization of the power-law parameters λ_2 and m. For both temperatures (215 and 230°C), for the λ_2 and m optimization, the software selected the entrance pressure loss data points for flow rates of 10.2 and 792 mm^3/s for the axisymmetric flow and for flow rates of 10.4 and 208 mm^3/s for the planar flow. Since the flow rates are similar for the axisymmetric and planar flows, it should be noted that strain rates are higher for the axisymmetric flow because the area of cross-section of the channel beyond the contraction is larger for the planar case. Since the entrance loss data was available at lower strain rates for the planar flow, the strain thickening portion of the elongational viscosity could only be captured for the planar flow. For optimization of the δ and λ_1 parameters for planar flow, the entrance loss data point for the flow rate of 10.4 mm^3/s was used for 215°C as well as for 230°C. With these control points, the elongational viscosity parameters predicted by the optimization software are as follows:

Axisymmetric flow
215°C: $\delta = 0$, $\lambda_2 = 2.18$ s, $m = 0.349$
230°C: $\delta = 0$, $\lambda_2 = 1.85$ s, $m = 0.349$

Planar flow
215°C: $\delta = 37.3$, $\lambda_1 = 2250$ s, $\lambda_2 = 46.2$ s, $m = 0.450$
230°C: $\delta = 37.3$, $\lambda_1 = 373$ s, $\lambda_2 = 39.2$ s, $m = 0.450$

For λ_1 optimization entrance loss at lower flow rates is required. However, at very low flow rates, entrance loss is too small to measure accurately. Therefore, the predicted values of the λ_1 parameter may not be very accurate.

It should be noted that the optimization software predicts the elongational viscosity parameter separately for each temperature. Except for the λ_1 values, which are not expected to be very accurate, the other three parameters were found to follow the time-temperature superposition principle. This observation is in agreement with the results of Munstedt and Laun [14]. Munstedt and Laun [14] used a Meissner-type uniaxial extension rheometer [15] to measure elongational viscosity at low elongation rates. They concluded that the slope of the elongational viscosity curve remains unaltered by a change in temperature and the time-temperature superposition can be used to shift elongational viscosity. Furthermore, they found that the temperature shift factors for elongational viscosity were

identical to those for shear viscosity, which is also true for the values of δ, λ_2 and m reported above.

Fig. 1 also shows the elongational viscosity predicted by Binding's analysis. To obtain the power-law parameters for elongational viscosity by Binding's analysis, the same two data points as those used for finding the optimal values of λ_2 and m were used. That is, the data points for flow rates of 10.2 and 792 mm^3/s for the axisymmetric flow and for flow rates of 10.4 and 208 mm^3/s for the planar flow were used. As expected, in the Newtonian and elongation-thickening portions of the elongational viscosity, the elongational viscosity predictions by Binding's analysis are much higher than the viscosity based upon the optimized values of the parameters in the Sarkar-Gupta model. In the power-law region, for the axisymmetric case, the predictions from Binding's analysis are in reasonable agreement with those from the present work. However, for the planar case, Binding's predictions are significantly higher than the elongational viscosity obtained by using the optimization software in the present work.

The axisymmetric elongational viscosity in Fig. 1 does not have any elongation-thickening region. However, the actual axisymmetric elongational viscosity may have an elongation-thickening region. Since the experimental entrance loss data is available only for higher flow rates, the elongation-thickening region for axisymmetric elongational viscosity could not be captured in the present work. It is evident from Fig. 1 that for Dow 132i, for the same value of e_{II}, the planar elongational viscosity is always larger than the axisymmetric elongational viscosity. It will be interesting to investigate in the future, if this observation is valid for other polymers as well.

Besides the experimental data, Figs. 2 and 3 also show the entrance loss predicted by our software. The curves labeled Sarkar-Gupta, in fact use the Sarkar-Gupta model for elongational viscosity along with the Carreau model for shear viscosity, whereas the curves labeled Carreau use the Carreau model with a generalized Newtonian formulation. For various parameters in these equations, the values given earlier in this section were used in the flow simulation. It is evident from Figs. 2 and 3 that the entrance loss predicted in the present work is in good agreement with the experimental data. The generalized Newtonian formulation with Carreau model predicted only about 25% of the experimental value of entrance pressure loss for axisymmetric flow and only about 10% of the experimental value for planar flow.

Conclusions

The planar and axisymmetric elongational viscosities of Dow 132i were estimated by minimizing the difference between the entrance loss predicted by a finite element simulation and the corresponding experimental data for the flow in slit and capillary rheometers. The planar and axisymmetric elongational viscosities were predicted for two different temperatures. The power-law regions of the planar and axisymmetric elongational viscosities were found to follow the time-temperature superposition principle. Since the experimental data at low flow rates, and hence the estimation of the elongational-thickening portion of the viscosity curve, is not highly accurate, the time-temperature superposition could not be verified for the elongational thickening region of the viscosity curve for planar flows. Because of the unavailability of the entrance loss data at low flow rates, the elongational thickening portion of the viscosity curve could not be captured for axisymmetric elongational viscosity.

References

1. R. B. Bird, R. C. Armstrong, and O. Hassager, *Dynamics of Polymeric Liquids*, Vol. 1 and 2, John Wiley, New York (1987).
2. P. J. Carreau, Ph.D. Thesis, University of Wisconsin, Madison (1968).
3. M. M. Cross, *J. Colloid Sci.,* **20**, 417 (1965).
4. C. A. Hieber (Chapter 1), A. I. Isayev, and R.K. Upadhyay (Chapter 2), in *Injection and Compression Molding Fundamentals*, A.I. Isayev, ed., Marcel Dekker (1987).
5. C.W. Maosko, *Rheology Principles, Measurements and Applications,* Wiley-VCH, New York (1994).
6. F. A. Morrison, *Understanding Rheology,* Oxford University Press, New York (2001).
7. M. Gupta, *Polym. Eng. Sci.,* **40**, 23 (2000).
8. F. N. Cogswell, *Polym. Eng. Sci.*, **12**, 64 (1972).
9. M. Gupta, *SPE ANTEC Tech. Papers*, **47**, 794 (2001).
10. D. M. Binding, *J. Non-Newtonian Fluid Mech.,* **27**, 193 (1988).
11. D. Sarkar and M. Gupta, in *CAE and Related Innovations for Polymer Processing*, L. S. Turng, H. P. Wang, K. Ramani and A. Bernard, eds., ASME MD-Vol. 90, 309 (2000).
12. W. H. Press, B. P. Flanery, S. A. Teukolsky and W. T. Vetterling, *Numerical Recipes*, Cambridge University Press, Cambridge (1989).
13. Datapoint Labs 95 Brown Road, Ithaca, NY 14850, USA (http://www.datapointlabs.com).
14. H. Munstedt, H. M. Laun. *Rheol. Acta*, **18**, 492 (1979).
15. J. Meissner, *Rheol. Acta.,* **8**, 78 (1969).
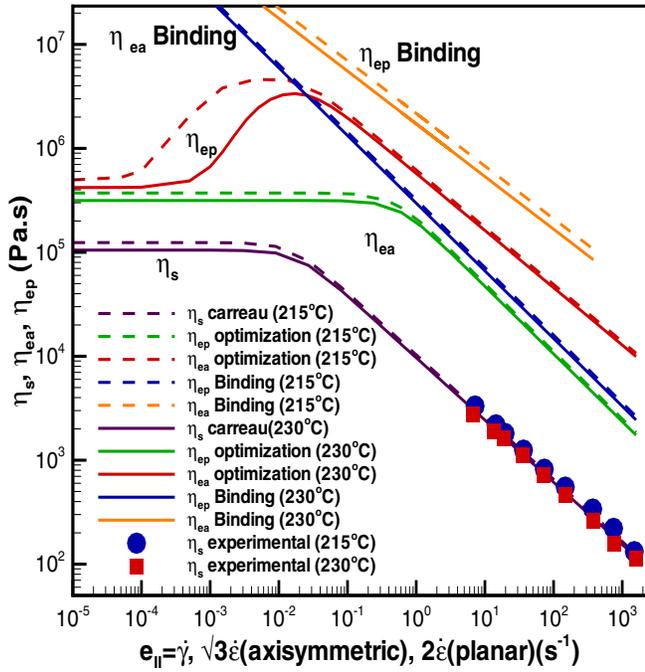
Fig. 1. Variation of shear (η_s) and elongational $(\eta_{ep}$ (planar), η_{ea} (axisymmetric)) viscosities of Dow 132i with the second invariant of strain-rate tensor (e_{II}).
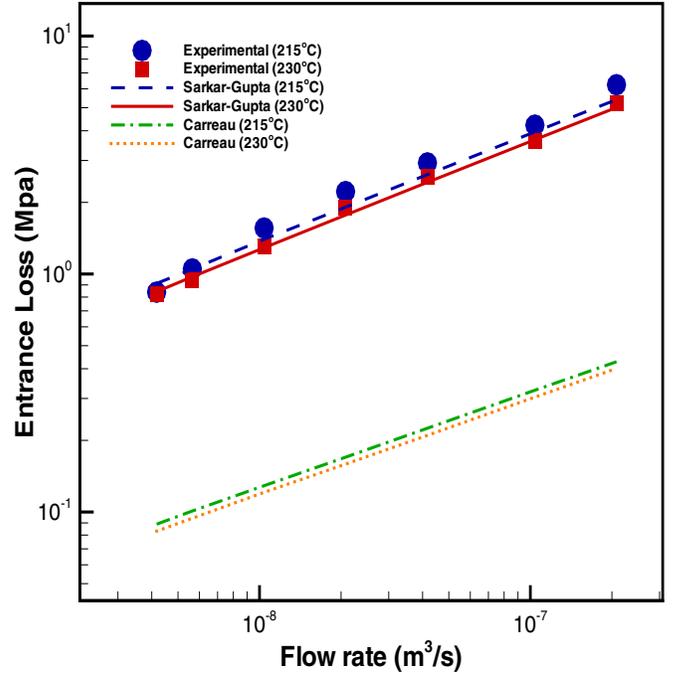
Fig 3. Entrance loss vs. flow rate for Dow 132i for planar flow.
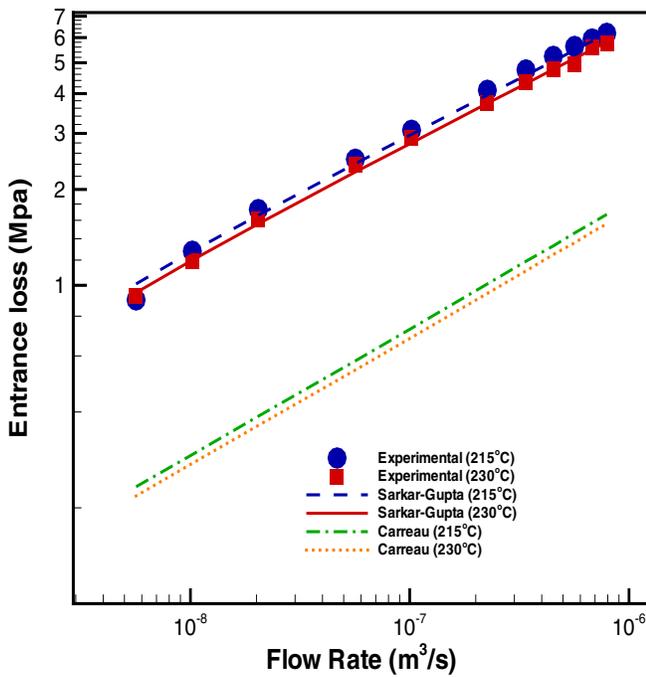
Fig. 2. Entrance loss vs. flow rate for Dow 132i for axisymmetric flow.